

---

# Accelerating Goal-Conditioned Reinforcement Learning Algorithms and Research

---

Michał Bortkiewicz<sup>1</sup> Włodek Pałucki<sup>2</sup> Vivek Myers<sup>3</sup>  
Tadeusz Dziarmaga<sup>4</sup> Tomasz Arczewski<sup>4</sup>  
Łukasz Kuciński<sup>2,5,6</sup> Benjamin Eysenbach<sup>7</sup>

<sup>1</sup>Warsaw University of Technology <sup>2</sup>University of Warsaw <sup>3</sup>UC Berkeley  
<sup>4</sup>Jagiellonian University <sup>5</sup>Polish Academy of Sciences <sup>6</sup>IDEAS NCBR <sup>7</sup>Princeton University  
michalbortkiewicz8@gmail.com wladek.palucki@gmail.com

## Abstract

Self-supervision has the potential to transform reinforcement learning (RL), paralleling the breakthroughs it has enabled in other areas of machine learning. While self-supervised learning in other domains aims to find patterns in a fixed dataset, self-supervised goal-conditioned reinforcement learning (GCRL) agents discover new behaviors by learning from the goals achieved during unstructured interaction with the environment. However, these methods have failed to see similar success, both due to a lack of data from slow environments as well as a lack of stable algorithms. We take a step toward addressing both of these issues by releasing a high-performance codebase and benchmark (JaxGCRL) for self-supervised GCRL, enabling researchers to train agents for millions of environment steps in minutes on a single GPU. The key to this performance is a combination of GPU-accelerated environments and a stable, batched version of the contrastive reinforcement learning algorithm, based on an infoNCE objective, that effectively makes use of this increased data throughput. With this approach, we provide a foundation for future research in self-supervised GCRL, enabling researchers to quickly iterate on new ideas and evaluate them in a diverse set of challenging environments.

Website + Code: <https://github.com/MichalBortkiewicz/JaxGCRL>

## 1 Introduction

Self-supervised learning has had a large impact on machine learning over the last decade, transforming how research is done in domains such as natural language processing and computer vision. In the context of reinforcement learning (RL), most self-supervised prior methods apply the same recipe that has been successful in other domains: learning representations or models from a large, fixed dataset. However, the RL setting also enables a fundamentally different type of self-supervised learning: rather than learning from a fixed dataset (as done in NLP and computer vision), a self-supervised reinforcement learner can collect its own dataset. Thus, rather than learning a representation of a dataset, the self-supervised reinforcement learner acquires a representation of an environment or of behaviors and optimal policies therein. Self-supervised reinforcement learners may address many of the challenges that stymie today’s foundations models: reasoning about the consequences of actions [10, 58, 83] (i.e., counterfactuals [51, 103]) and long horizon planning [25, 42, 103].

In this paper, we study self-supervised reinforcement learning in an online setting: an agent interacts in an environment without a reward to learn representations or models, which are later used to quickly solve downstream tasks. We refer to such interactions as “self-supervised” or “unlabeled” because the agent does not receive any reward feedback. We will focus on goal-conditioned algorithms,

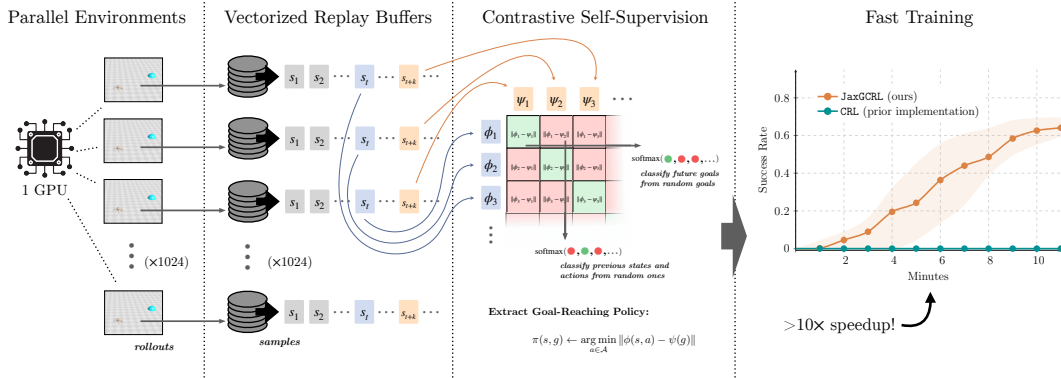


Figure 1: JaxGCRL learns goal-reaching policies for Ant in about 10 minutes on 1 GPU. This paper releases a GCRL benchmark and baseline algorithms that enable research and experiments to be done in minutes.

which aim to use these unsupervised interactions to learn a policy for reaching different goals. Prior work has proposed several prior algorithms for self-supervised RL [32, 73, 74, 110], including algorithms that focus on learning goals [26]. Yet, so far these methods have not yet provided the sort of foundational building block that self-supervised learning in other domains has provided; we have yet to see the same sort of emergent properties from self-supervised RL that we have seen from (say) self-supervised NLP (e.g., in-context learning).

The key barrier to realizing effective self-supervised RL algorithms is scale – algorithms and implementations that can collect extraordinarily large quantities of data and stably learn from that data. Self-supervised learning in other domains already requires vast quantities of data to achieve excellent performance [49, 72, 88], and we expect that even more experience will be required when RL agent has to interactively collect its own data. The main aim of this paper is to remove this barrier, providing extremely fast simulators that are tightly integrated with simple and scalable self-supervised RL algorithms. Simultaneously, we aim to build a framework that is broadly accessible, avoiding the complexity of distributed training, and not requiring more than a single GPU.

To achieve this goal, we will combine insights from self-supervised RL with recent advances in GPU-accelerated simulation. The first key ingredient is recent work on GPU-accelerated simulators, both for physics [36, 61, 100] and other tasks [12, 21, 34, 67, 86], enable users to collect data at almost 200,000 steps per second on a single 24GB GPU, 100× to 1000× faster [36] than prior methods based on CPUs, depending on the number of available CPU threads. While prior CPU-based methods can be parallelized to accelerate data collection, parallelization introduces complexity (e.g., distributed workers, multi-processing). GPU-accelerated simulators not only decrease the cost of data collection but also decrease the cost of performing gradient updates; since data from the simulator is already on the GPU, there is no need for copying data from CPU to GPU, which tends to be a bottleneck for modern GPUs [69]. The second key ingredient is a highly stable algorithm for self-supervised learning: an issue that causes training instability once every million observations is ignorable when training for  $10^6$  steps, but catastrophic if training for  $10^9$  steps. To address this, we build upon recent work on contrastive RL (CRL) [32, 110], which use temporal contrastive learning to learn a value function. The third key ingredient is a suite of tasks for evaluating self-supervised RL agents which is not only blazing fast, but which also stress tests the exploration and long-horizon reasoning capabilities of RL policies.

The key contribution of this work is a codebase that provides a highly stable implementation of self-supervised RL that is tightly integrated with a GPU-accelerated suite of environments. On a single GPU, an experiment with 10 million environment steps lasts only around 10 minutes, which is more than 10× faster than in the original CRL codebase [32] (Fig. 1). While the new benchmark environments demonstrate that existing self-supervised RL algorithms are more capable than previously believed, they also highlight several opportunities for algorithmic improvement.

This paper is not just about a particular algorithm or set of environments, but starts getting at key questions about how RL is taught and how RL research is done. The speed of experiments will allow researchers to interactively debug their algorithms, changing pieces and getting results in a matter of minutes; algorithm design may look more like data science than rocket science. The new

codebase will make RL more accessible not just by making installation easy (one set of dependencies for the algorithms and environments), but by allowing students at less-resourced schools to run “real” experiments on a single GPU in minutes; a free Colab GPU instance resetting once per hour is much less frustrating if each experiment completes in a few minutes. Finally, the codebase may help make RL research more reproducible (less costly to run many random seeds) while also helping to address the “war of attrition” in several areas of RL, whereby the labs with the most compute produce the best methods simply because they can do the most hyperparameter optimization or run their algorithms for the most number of environment steps.

For researchers, the speed of experiments will allow them to “interactively” debug their algorithms, changing pieces and getting results in near real time. Finally, this repository will break down barriers to RL research, enabling researchers from less resourced schools and institutions to get involved in state-of-the-art RL research.

## 2 Related Work

Our new benchmark and implementation build upon recent advances in goal-conditioned reinforcement learning (GCRL), showing that scalable contrastive learning algorithms can be combined with hardware-accelerated environments to enable fast and stable training of self-supervised RL agents across a suite of benchmarks.

### 2.1 Goal-Conditioned Reinforcement Learning

Goal-conditioned reinforcement learning is a special case of the general multi-task reinforcement learning setting, in which the potential tasks in an environment defined by goal states in the environment that the agent is trying to reach [38, 54, 77]. Formally, the GCRL setting augments a Markov decision process (MDP) with a potential reward function (the indicator function) for each possible goal state in the MDP [32]. Being able to reach any possible goal is a particularly attractive as an objective for learning generalist agents: arbitrary goals can express diverse behaviors in the environment and do not require a hand-specified reward function for each task (every state specifies a task when viewed as a goal) [89]. GCRL techniques have seen success in domains such as robotic manipulation [2, 24, 31, 39, 106] and navigation [47, 60, 66, 92]. Recent work has shown that representations of goals can be imbued with additional structure to enable capabilities such as language grounding [64, 74], compositionality [63, 75, 107], and planning [30, 80]. In this paper, we show how GCRL techniques based on contrastive learning [32] can be scaled with GPU-acceleration to enable fast and stable training.

### 2.2 Accelerating Deep Reinforcement Learning

Deep RL has only recently become practical for many tasks, in part due to improvements in hardware support for these algorithms. Distributed training has enabled RL algorithms to scale across hundreds of GPUs [27, 28, 48, 70]. To resolve the bottleneck of environment interaction with CPU-bound environments, various GPU accelerated environments have been proposed [12, 21, 36, 61, 65, 67, 86]. In addition to reducing CPU-GPU data-transfer overhead, these environments can easily be vectorized with frameworks like Jax [14, 44, 46] to collect data from hundreds of rollouts in parallel. In this paper, we leverage these advances with a modified contrastive RL algorithm to scale self-supervised GCRL across orders of magnitude more data than previously possible.

### 2.3 Self-Supervised RL and Intrinsic Motivation

Self-supervised training has enabled key breakthroughs in language modeling and computer vision [23, 43, 68, 91, 112]. In the context of RL, we will use the term self-supervised to mean techniques that can learn through interaction with an environment without a reward signal. Perhaps the most successful form of self-supervision here have been in multi-agent games that can be rapidly simulated, such as Go and Chess, where self-play has enabled the creation of superhuman agents [94, 95, 97, 109]. When learning goal-reaching agents, another basic form of self-supervision is to relabel trajectories as successful demonstrations of the goal that was reached, even if it differs from the original commanded goal [54, 105]. This technique has seen recent adoption under the term “hindsight experience” replay for various deep RL algorithms [2, 17, 32, 39, 84].

Another perspective on self-supervision is intrinsic motivation, broadly defined as when an agent computes its own reward signal, ideally relating to some notion of desirable behavior [6]. Intrinsic motivation methods include curiosity [6–8], surprise minimization [9, 85], and empowerment [20, 22, 56, 73, 87]. Closely related are skill discovery methods, which aim to construct intrinsic rewards for diverse collections of behavior [29, 40, 55, 59, 79, 81, 93]. Self-supervised and unsupervised reinforcement learning methods have been historically difficult to scale due to the need for large numbers of environment interactions [35, 71]. With this work, we aim to address this bottleneck by providing a fast and scalable implementation and algorithm for contrastive, self-supervised RL on a benchmark of diverse tasks.

## 2.4 RL Benchmarks

The RL community has recently started to pay greater attention to how RL research is conducted, reported and evaluated [1, 45, 52]. A key issue is a lack of reliable and efficient benchmarks—it becomes hard to rigorously compare novel methods when the number of trials needed to see statistically significant results across diverse settings ranges in the thousands of training hours [53]. Some benchmarks that *have* seen adoption include OpenAI gym [15], the DeepMind Control Suite [98], D4RL [37]. More recently, hardware-accelerated versions of some of these benchmarks have been proposed [41, 57, 65, 67]. Our contribution is to propose a stable contrastive algorithm and suite of goal-reaching tasks that can enable meaningful RL research on a single GPU by significantly reducing the cost of running experiments.

## 3 Self-Supervision through Goal-Conditioned Reinforcement Learning

In the goal-conditioned reinforcement learning setting, an agent interacts with a controlled Markov process (CMP)  $\mathcal{M} = (\mathcal{S}, \mathcal{A}, p, p_0, \gamma)$  to reach arbitrary goals [2, 11, 54]. At any time  $t$  the agent will observe a state  $s_t$  and select a corresponding action  $a_t \in \mathcal{A}$ . The dynamics of this interaction are defined by the distribution  $p(s_{t+1} | s_t, a_t)$ , with an initial distribution  $p_0(s_0)$  over the state at the start of a trajectory, for  $s_t \in \mathcal{S}$  and  $a_t \in \mathcal{A}$ . For any goal  $g \in \mathcal{S}$ , we cast optimal goal-reaching as a problem of inference [5, 11, 13, 32]: given the current state and desired goal, what is the most likely action that will bring us toward that goal? As we will see, this is equivalent to solving the Markov decision process (MDP)  $\mathcal{M}_g$  obtained by augmenting  $\mathcal{M}$  with the goal-conditioned reward  $r_g$ :

$$r_g(s_t, a_t) = p(g | s_t, a_t).$$

Formally, a goal-conditioned policy  $\pi(a | s, g)$  receives both the current observation of the environment as well as a goal observation  $g \in \mathcal{S}$ . We inductively define the  $k$ -step (action-conditioned) policy visitation distribution:

$$\begin{aligned} p_1^\pi(s_1 | s_0, a_0) &\triangleq p(s_1 | s_0, a_0), \\ p_{k+1}^\pi(s_{k+1} | s_0, a_0) &\triangleq \int_{\mathcal{A}} \int_{\mathcal{S}} p(s_{k+1} | s, a) dp_k^\pi(s | s_0, a_0) d\pi(a | s) \\ p_{k+t}^\pi(s_{k+t} | s_t, a_t) &\triangleq p^\pi(s_k | s_0, a_0). \end{aligned}$$

We define the discounted state visitation distribution as  $p_\gamma^\pi(s^+ | s, a) \triangleq \sum_{k=0}^{\infty} \gamma^k p_k^\pi(s^+ | s, a)$ , which we interpret as the distribution of the state  $K$  steps in the future for  $K \sim \text{Geom}(1 - \gamma)$ . This last expression is precisely the  $Q$ -function of the policy  $\pi(\cdot | \cdot, g)$  for the reward  $r_g$ :  $Q_g^\pi(s, a) \triangleq p_\gamma^\pi(g | s, a)$  [32]. For a given distribution over goals  $g \sim p_G$ , we can now write the overall objective as

$$\max_{\pi(\cdot | s, g)} \mathbb{E}_{p_0(s_0)p_G(g)\pi(a_0 | s_0, g)} [p_\gamma^\pi(g | s_0, a_0)]. \quad (1)$$

### 3.1 Contrastive Representations for Goal-Reaching

Equation (1) tells us that to optimally reach goals  $g \in \mathcal{S}$ , we should learn a policy

$$\pi^*(a | s, g) = \arg \max_{\pi(a | s, g)} p_\gamma^\pi(g | s, a).$$

This suggests that we can learn an optimal goal-reaching policy by learning and maximizing a critic  $f(s, a, g) \propto p_\gamma^\pi(g | s, a)$  with respect to the actions  $a$ .

We extend a long line of work that views learning this critic as a classification problem [31–33, 75, 110, 111], training this critic on batches of  $(s, a, g)$  to classify whether  $g$  is the goal state of the trajectory  $(s, a)$ , or whether it is a negative sample. In Section 5.4, we will discuss variants of this contrastive loss. The base contrastive loss we study will be the infoNCE objective [96], modified to use a symmetrized [82] critic parameterized with  $\ell_2$ -distances [30].

To learn the critic, we will first define two additional state-marginal measures:

$$p_S(s) = \int_S \int_{\mathcal{A}} p(s | s, a) d\pi(a | s) dp_0(s)$$

$$p_S^+(s^+) = \int_S \int_{\mathcal{A}} p(s^+ | s, a) d\pi(a | s) dp_S(s).$$

As we train  $\pi$ , we will sample batches  $\mathcal{B}$  from a replay buffer  $\mathcal{D}$ . Assuming  $\pi$  is fixed and that resets occur with probability  $(1 - \gamma)$ , we can write the distribution over  $(s, a, g)$  values sampled in the batch as

$$\mathcal{B} \leftarrow \{(s_i, a_i, g_i)\}_{i=1}^K \sim p_S(s)\pi(a | s)p_\gamma^\pi(g | s, a).$$

The family of contrastive RL algorithms Eysenbach et al. [29, 30], consists of the following components: (a) the state-action pair and goal state representations,  $\phi(s, a)$  and  $\psi(g)$ , respectively; (b) the critic, which is defined as an energy function  $f_{\phi, \psi}(s, a, g)$  and the loss function; and (c) a contrastive loss function, which is a function of the matrix containing the critic values  $\{f_{\phi, \psi}(s_i, a_i, g_j)_{i,j}\}$ , related to the elements of the batch  $\mathcal{B}$ . Section 5.1 contain the formulas for the choices considered in this paper.

### 3.2 Policy Learning

We use a DDPG-style policy extraction loss to learn a goal-conditioned policy with this critic [62]. Parameterizing the policy as some  $\pi_\theta(a | s, g)$ , we get

$$\mathcal{L}_{\text{policy}}(\mathcal{B}; \theta) = \sum_{i,j=1}^K \int_{\mathcal{A}} f_{\phi, \psi}(s_i, a_i, g_j) d\pi_\theta(a_i | s_i, g_i). \quad (2)$$

Breaking with prior contrastive RL approaches [32], we sample goals from the same trajectories as the states and actions, which we find improves performance (see Appendix C for more discussion). The overall objectives then become

$$\min_{\phi, \psi} \mathbb{E}_{\mathcal{B} \sim \mathcal{D}} [\mathcal{L}_{\text{infoNCE}}(\mathcal{B}; \phi, \psi)] \quad \text{and} \quad \min_{\theta} \mathbb{E}_{\mathcal{B} \sim \mathcal{D}} [\mathcal{L}_{\text{policy}}(\mathcal{B}; \theta)].$$

## 4 New Implementation and Benchmark

The key contribution of this paper is the extremely fast implementation of state-based self-supervised reinforcement learning algorithms and a new benchmark of BRAX-based [36] environments. Our implementation leverages the power of GPU-accelerated simulators to reduce the time required for data collection and training, allowing researchers to run extensive experiments in a fraction of the time previously needed. The bottleneck of former self-supervised RL implementations was twofold. Firstly, data collection was executed on many CPU threads, as a single thread was often used for a single actor. This reduced the number of possible parallel workers, as only high-compute servers could run hundreds of parallel actors. Secondly, the necessity of data migration between CPU (data collection) and GPU (training) posed additional overhead. These two problems are mitigated by fully jittable algorithm implementation and environments running directly on GPU. We provide a robust framework that showcases the potential of self-supervised RL and offers a practical tool for the community to develop and evaluate new algorithms efficiently.

For instance, testing design choices such as new contrastive loss or energy function could be completed in less than 30 minutes, with ten of those dedicated to implementation. We tested several recent contrastive learning ideas during the framework’s development, such as Eysenbach et al. [32]. Having results ready within half an hour after reading a paper or brainstorming is a radically different workflow from how RL research has been done over the last few years.

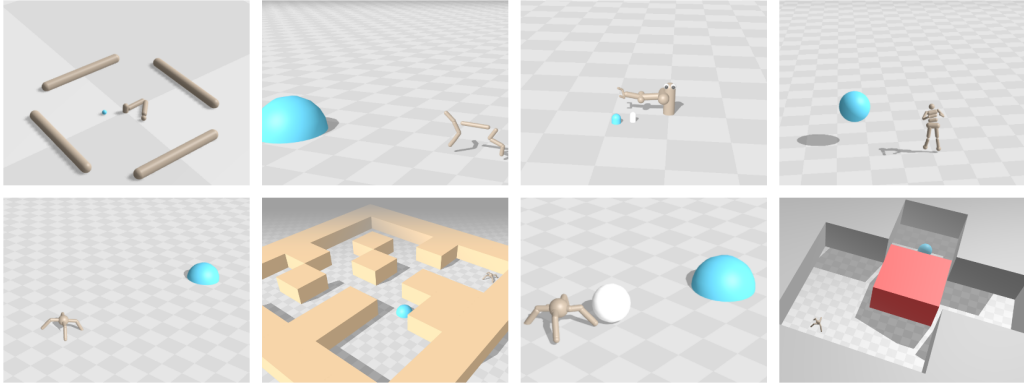


Figure 2: JaxGCRL: We release a new suite of GPU-accelerated environments and algorithms for studying goal-conditioned RL. The agent does not receive any rewards or demonstrations, making some of these tasks an excellent testbed for studying exploration and long-horizon reasoning. Our accompanying implementation of GCRL algorithms trains at up to 10,000 steps per second on a single GPU, enabling rapid experimentation.

#### 4.1 Training speedup from environment vectorization on a single GPU

To evaluate the speedup of the proposed implementation, we execute the basic goal-conditioned contrastive RL method [32] using original and novel repositories. We conducted experiments using a 16:1 ratio of environment steps to neural network updates, as the initially suggested 1:1 ratio led to lower performance, perhaps due to excessive updates per environment step.

In Fig. 1, we report the performance of the CRL agent in Ant environment and the wall-clock time of the experiment. In particular, we report results for CRL agent that uses the NCE-binary objective with a dot-product critic, the main configuration from [32]. The experiments were carried out on an NVIDIA V100 GPU. The speedup in this configuration is 22-fold. Further speedup results are presented in Appendix A.1. Notably, our implementation uses only one CPU thread and has low RAM usage as all the operations, including those on the replay buffer, are computed on GPU.

#### 4.2 Benchmark

To evaluate the performance of our methods, we propose a new goal-conditioned task benchmark consisting of eight diverse continuous control environments. These environments range from very easy ones, suitable for sanity checks, to complex, exploration-oriented tasks. All environments are implemented in JAX and can be run on accelerated hardware, enabling the collection of trajectories from thousands of environment instances in parallel. When selecting environments, we aimed to include tasks that require not only spatial navigation but also an understanding of the spatial layout and object manipulation through agent interaction.

The list below includes a short description of each environment, with technical details for each environment in Table 1:

- Reacher** [15] This is a simple 2d manipulation task, the goal is to have end part of a 2-segment robotic arm in a specific place. The goal location is sampled uniformly from a disk around an agent.
- Half Cheetah** [108] In this 2d task, a 2-legged agent has to get to a goal that is sampled from one of the 2 possible places, one on each side of the starting position.
- Pusher** [15] This is a 3d robotic task, that consists of a robotic arm and a movable circular object resting on the ground. The goal is to use the arm to push the object into the goal position. With each reset both position of the goal and movable object are selected randomly. We prepared two variants of this task, an *easy* version, where object and goal start closer to each other, and a *hard* version, where they are further apart.

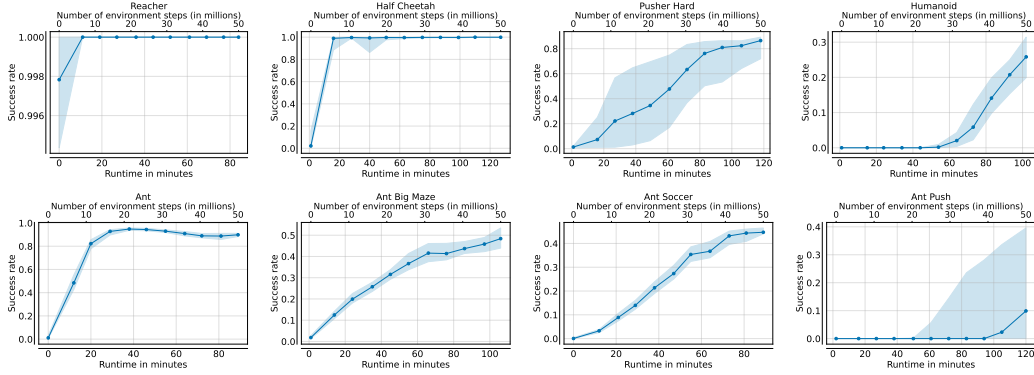


Figure 3: Success rates for each of our benchmark environments. Reported as IQM of 10 seeds.

**Ant** [90] This is a re-implementation of classic Mujoco Ant task. A quadruped robot has to walk to the goal that is sampled uniformly from a circle with center at the starting position.

**Ant Maze** [37] This environment uses the same quadruped model as the previous Ant, but the agent must navigate a maze to reach the target. We prepared 3 different mazes varying in size and difficulty. In each maze the goals are sampled from a set of listed possible positions.

**Ant Soccer** [102] In this environment the Ant has to push a spherical object into a goal position that is sampled uniformly from a circle around the starting position. The position of the movable sphere is set to be on the line between an agent and a goal, with some random noise added.

**Ant Push** [76] To reach a goal, the Ant model has to push a movable box out of the way. If the box is pushed in the wrong direction, the task becomes impossible to complete.

**Humanoid** [99] This is another classic Mujoco task. The model has to navigate a complex humanoid-like robot to walk towards a goal sampled from a disk with a center at the starting position.

In Fig. 3, we report the baseline results for the proposed benchmark. Notably, we are able to train big CRL agents (with four hidden layers, each with 1024 neurons) in high-dimensional tasks such as ant and humanoid in less than 2 hours. The detailed setup is presented in Section 5.8.

## 5 Empirical Experiments with JaxGCRL

We ablated the key components of the CRL algorithm across the environments in our benchmark to stabilize and improve its performance. These experiments were made possible by our hardware-accelerated environments and batched contrasting learning implementation, which allowed us to train hundreds of agents over millions of environment steps in a few hours.

### 5.1 Contrastive RL design choices

**Energy functions** Measuring the similarity between samples could be achieved in various ways, including cosine similarity [19], dot product [82], and negative  $L_1$  and  $L_2$  distance [50]. Namely,

$$f_{\phi, \psi, \text{cos}}(s, a, g) = \frac{\langle \phi(s, a), \psi(g) \rangle}{\|\phi(s, a)\|_2 \|\psi(g)\|_2}, \quad (3)$$

$$f_{\phi, \psi, \text{dot}}(s, a, g) = \langle \phi(s, a), \psi(g) \rangle, \quad (4)$$

$$f_{\phi, \psi, L_1}(s, a, g) = -\|\phi(s, a) - \psi(g)\|_1, \quad (5)$$

$$f_{\phi, \psi, L_2}(s, a, g) = -\|\phi(s, a) - \psi(g)\|_2, \quad (6)$$

$$f_{\phi, \psi, L_2 w \setminus o \text{ sqr t}}(s, a, g) = -\|\phi(s, a) - \psi(g)\|_2^2. \quad (7)$$

Even though there is no consensus on the choice of energy functions for temporal representations in CRL, recent works showed that they should abide by quasimetric properties [75, 107].

**Contrastive losses** In addition to different parameterizations for the energy function, we also can vary the loss function with which the energy function is trained. In particular, we evaluate InfoNCE [32, 104]-type losses, FlatNCE [18]-type losses, Monte Carlo version of Forward-Backward unsupervised loss [101], and losses inspired by preference optimization for Large Language Models[16]. More precisely, we tested the following losses:

$$\mathcal{L}_{\text{InfoNCE\_forward}}(\mathcal{B}; \phi, \psi) = - \sum_{i=1}^K \log \left( \frac{e^{f_{\phi, \psi}(s_i, a_i, g_i)}}{\sum_{j=1}^K e^{f_{\phi, \psi}(s_i, a_i, g_j)}} \right), \quad (8)$$

$$\mathcal{L}_{\text{InfoNCE\_backward}}(\mathcal{B}; \phi, \psi) = - \sum_{i=1}^K \log \left( \frac{e^{f_{\phi, \psi}(s_i, a_i, g_i)}}{\sum_{j=1}^K e^{f_{\phi, \psi}(s_j, a_j, g_i)}} \right), \quad (9)$$

$$\mathcal{L}_{\text{InfoNCE\_symmetric}}(\mathcal{B}; \phi, \psi) = \mathcal{L}_{\text{InfoNCE\_forward}}(\mathcal{B}; \phi, \psi) + \mathcal{L}_{\text{InfoNCE\_backward}}(\mathcal{B}; \phi, \psi), \quad (10)$$

$$\mathcal{L}_{\text{DPO}}(\mathcal{B}; \phi, \psi) = - \sum_{i=1}^K \sum_{j=1}^K \log \sigma [f_{\phi, \psi}(s_i, a_i, g_i) - f_{\phi, \psi}(s_i, a_i, g_j)], \quad (11)$$

$$\mathcal{L}_{\text{IPO}}(\mathcal{B}; \phi, \psi) = \sum_{i=1}^K \sum_{j=1}^K [(f_{\phi, \psi}(s_i, a_i, g_i) - f_{\phi, \psi}(s_i, a_i, g_j)) - 1]^2, \quad (12)$$

$$\mathcal{L}_{\text{SPPO}}(\mathcal{B}; \phi, \psi) = \sum_{i=1}^K \sum_{j=1}^K [f_{\phi, \psi}(s_i, a_i, g_i) - 1]^2 + [f_{\phi, \psi}(s_i, a_i, g_j) + 1]^2, \quad (13)$$

$$\mathcal{L}_{\text{FlatNCE\_forward}}(\mathcal{B}; \phi, \psi) = - \sum_{i=1}^K \log \left( \frac{\sum_{j=1}^K e^{f_{\phi, \psi}(s_i, a_i, g_j) - f_{\phi, \psi}(s_i, a_i, g_i)}}{\text{detach}[\sum_{j=1}^K e^{f_{\phi, \psi}(s_i, a_i, g_j) - f_{\phi, \psi}(s_i, a_i, g_i)}]} \right), \quad (14)$$

$$\mathcal{L}_{\text{FlatNCE\_backward}}(\mathcal{B}; \phi, \psi) = - \sum_{i=1}^K \log \left( \frac{\sum_{j=1}^K e^{f_{\phi, \psi}(s_j, a_j, g_i) - f_{\phi, \psi}(s_i, a_i, g_i)}}{\text{detach}[\sum_{j=1}^K e^{f_{\phi, \psi}(s_j, a_j, g_i) - f_{\phi, \psi}(s_i, a_i, g_i)}]} \right), \quad (15)$$

$$\mathcal{L}_{\text{FB}}(\mathcal{B}; \phi, \psi) = - \sum_{i=1}^K (e^{f_{\phi, \psi}(s_i, a_i, g_i)}) + \frac{1}{2(K-1)} \sum_{i=1}^K \sum_{j=1, j \neq i}^K (e^{f_{\phi, \psi}(s_i, a_i, g_j)})^2 \quad (16)$$

where we have highlighted the indices corresponding to **positive** and **negative** samples for clarity. Such a wide array of diverse losses not only allows us to test how well each particular loss performs but also shows the robustness of Contrastive Reinforcement Learning as a general method.

**Architecture scaling.** While scaling architectures is commonplace in other areas of ML, it is still unclear the right way to scale RL models, mainly because RL objectives are primarily defined as regression rather than easier to train with deep architectures classification [33]. Recently, Zheng et al. [110] showed that CRL might benefit from deeper and wider architectures for offline CRL in pixel-based environments; we want to examine whether this also holds for online state-based settings.

**Layer Normalization.** Recently, several design choices were thoroughly evaluated and incorporated into neural networks used for function approximation and policy in RL [78, 110]. Interestingly, one of the most potent design choices is layer normalization [3] for every hidden layer. The current understanding of layer normalization [4] is that it mitigates catastrophic overestimation by bounding the Q-values for actions even outside the offline dataset.

We evaluate these design choices in the following sections using the proposed codebase and benchmark. We note that the primary goal of experiments is to establish a strong baseline on the proposed environments through a solid examination of well-known methods.

## 5.2 Experimental Setup

Our experiments use a suite of simulated environments described in Section 4.2. We evaluate CRL in an online setting, with a ratio of network updates to environment steps equal to 1:16, using a batch size of 256 and a discount factor of 0.99. For every environment, we sample evaluation goals from the same distribution as training ones and use a replay buffer of size 10M. We use 1024

parallel environments to gather the data and run experiments for 50M environment steps. In every environment, we use a tuneable entropy coefficient.

*First*, in sections Sections 5.3 to 5.6, we try to understand the influence of design choices on learning performance. *Second*, in Section 5.8 we aggregate the proposed choices into the most effective algorithm to establish baseline results on our suite of goal-conditioned environments.

### 5.3 Energy Function Comparison

The performance of contrastive learning is sensitive to energy function choice [96]. This section aims to understand how different energy functions impact CRL performance. In particular, we evaluate five energy functions: L1, L2, L2 w/o sqrt, dot product and cosine. For every energy function, we use symmetric InfoNCE as a contrastive objective, with a 0.1 logsumexp penalty coefficient.

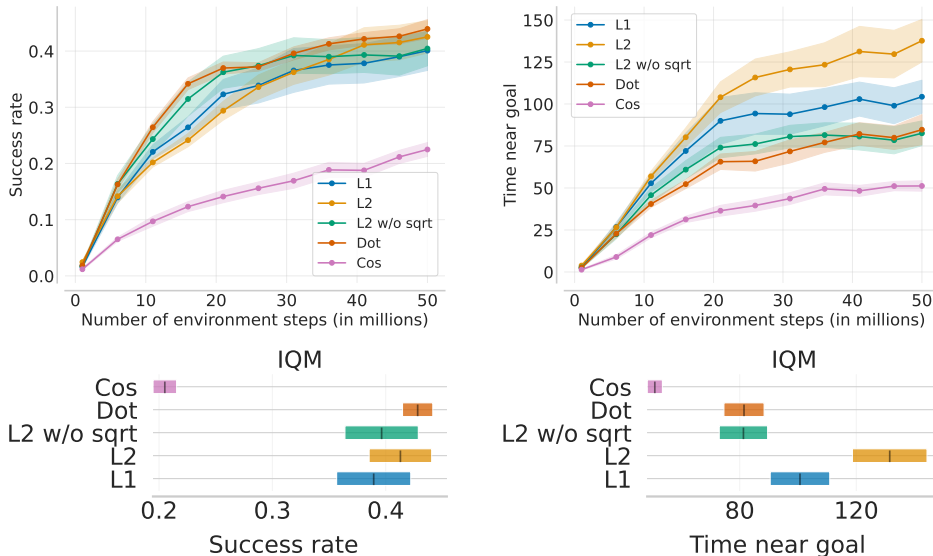


Figure 4: Success rate (left) and time near goal (right) results for different energy functions. Sample efficiency curves (top) and IQMs (bottom) indicate better performance of p-norms and dot product as energy functions over cosine similarity for CRL. Results averaged over five seeds.

In Fig. 4, we report the performance of every energy function for four different ant environments and pusher. We find that p-norms and dot-product significantly outperform cosine similarity. Additionally, removing the root square from the L2 norm (L2 w/o sqrt) results in performance degradation, especially regarding time near goal. This modification makes the energy function no longer abide by the triangle inequality, which, as pointed out by [75], is desirable for temporal contrastive features. Results per environment are reported in Appendix A.2.

### 5.4 Contrastive losses comparison

Next, we study the efficacy of contrastive losses on the same set of environments as energy functions. The baseline contrastive loss used in the original CRL implementation was the NCE-binary objective. We compare it with five other objectives: InfoNCE, InfoNCE Backward, Symmetric InfoNCE, FlatNCE and FlatNCE Backward. We use a logsumexp penalty equal to 0.1 for every objective, as without this auxiliary objective, InfoNCE collapses.

In Fig. 5, we observe that the originally used NCE-binary objective, forward-backward, IPO and SPPO are the worst-performing ones among tested objectives. However, among the other InfoNCE-derived objectives, it is difficult to determine the best one, as their performance is similar. Interestingly, contrastive RL seems fairly robust to the choice of loss objective.

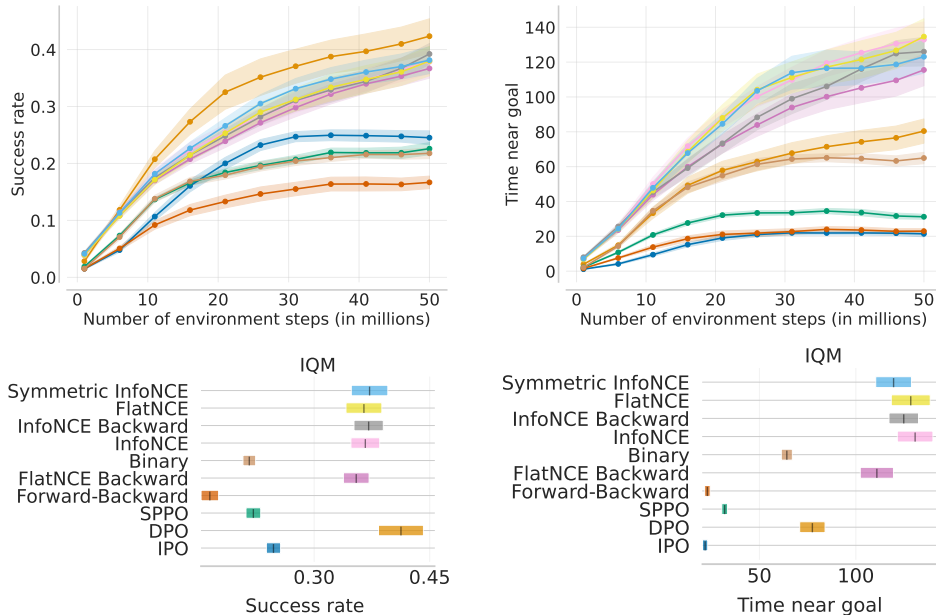


Figure 5: Effect of different contrastive loss functions on the CRL performance. The best performing are InfoNCE-derived loss functions and DPO regarding success rates. However, DPO results in a lower cumulative time near the goal. Results averaged over 10 seeds.

### 5.5 Scaling the Architecture

In this section, we examine how simply scaling up actor and critic neural networks in terms of depth and width impacts CRL performance. We evaluate the performance in four environments: Ant, Ant Soccer, and Ant U-Maze. We use the L2 energy function and Symmetric InfoNCE contrastive loss in every agent, with a logsumexp penalty equal to 0.1.

In Fig. 6, we report success rate averaged metrics of the last 10M steps in runs of length 50M environment steps. There is a clear trend of improving performance with depth for hidden layers with 256 and 512 neurons. However, this trend breaks for 4 hidden layers with 1024 neurons. This indicates training destabilization while naively scaling architecture. In Section 5.6, we show that simply adding Layer Normalization [3] before every activation allows better scaling, even for deep and wide architectures.

### 5.6 Effect of layer normalization

As shown in Fig. 7, for state-based CRL, we also observe the positive effects of this intervention. The probability of method performance improvement increases with the width and depth of the neural network. Additionally, in Fig. 8, we plot the aggregated performance of the neural network with 4 hidden layers and 1024 neurons in each, which obtained low results while naively scaling in Section 5.5. We obtain the best-performing architecture from the tested ones by adding Layer Normalization.

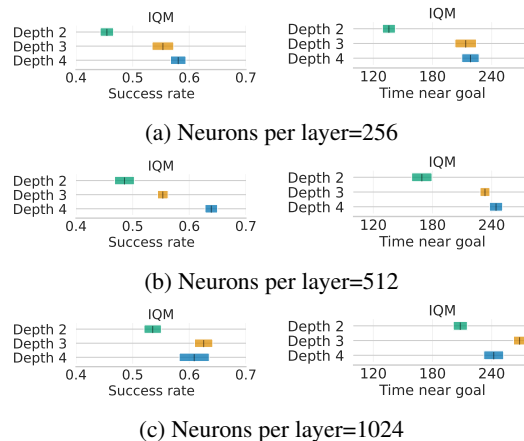


Figure 6: Impact of neural network depth and width on aggregated success rate and time near goal. We report aggregated metrics for the last 10M steps over 3 Ant environments (5 seeds per configuration).

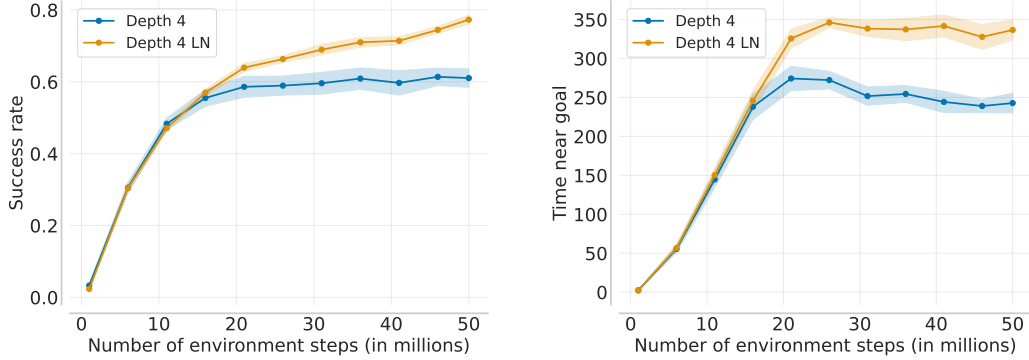


Figure 8: Performance improvement while using Layer Normalization for the deepest and widest architecture for aggregated envs. Adding Layer Normalization enables further architecture scaling.

### 5.7 Scaling the data

In Fig. 9, we report performance for different combinations of energy functions and contrastive objectives in a big data setup. In particular, we train the best-performing architecture from the previous section for 300 million environment steps in Ant and Ant U-Maze environments. We observe that the L2 energy function with InfoNCE objective and 0.1 logsumexp penalty configuration outperforms all others by a substantial margin, resulting in a much higher success rate and time near the goal in both tasks. This indicates that only a subset of a wide array of design choices performs well in effectively scaling Contrastive RL.

### 5.8 Benchmark baselines

After establishing the best-performing variant for key hyperparameters, we tested the performance of our method with configuration, including all of the improvements from previous sections. Final hyperparameter configuration for benchmark included Symmetric InfoNCE loss, L2 energy function with 0.1 logsumexp\_penalty, full configuration can be found in Table 2. Each environment was tested on 10 seeds, and the values reported in Fig. 3 are the Interquartile Mean (IQM) and standard error. Humanoid environment was trained on goals sampled from the distance in range [1.0, 5.0] meters and evaluated on goals sampled from distance 5.0 meters. All other environments were trained and evaluated on identical environments.

## 6 Conclusion

In this paper, we proposed very fast benchmark and baselines for goal-conditioned RL. The speed of the new benchmark enables us to rapidly study design choices for state-based CRL,

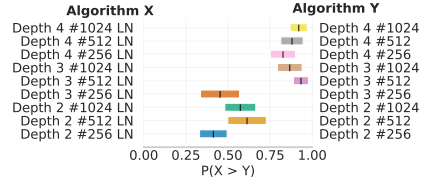


Figure 7: The probability of success rate improvement while using Layer Normalization depends on the architecture size.

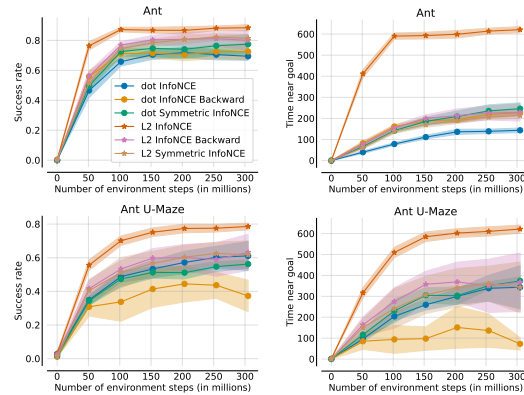


Figure 9: Effect of data scale on Ant and Ant U-Maze environments for different combinations of energy function and contrastive objective. Among tested configurations, L2 with InfoNCE objective scales up the best with a big amount of data.

including the network architectures and contrastive losses. We expect that self-supervised RL methods will open the door to entirely new learning algorithms with broad capabilities that go beyond the capabilities of today’s foundational models. The key step towards this goal is accelerating and democratising self-supervised RL research so that any lab can carry it out regardless of its computing capabilities. Open-sourcing the proposed codebase with easy-to-implement self-supervised RL methods is an important step in this direction.

**Limitations.** Our benchmark environments and methods assume full observability and that goals can be sampled from a goal distribution during training rollouts. Future work should relax these assumptions, which are common in practical settings where self-supervised RL agents might be useful. We also only investigate the online setting. Future work could examine hardware-accelerated environments and algorithms in the offline setting.

**Acknowledgments.** We gratefully acknowledge Polish high-performance computing infrastructure PCSS PLCloud for providing computer facilities and support within computational grant no. pl0334-01. We gratefully acknowledge Poland’s high-performance Infrastructure PLGrid (HPC Center: ACK Cyfronet AGH) for providing computer facilities and support within computational grant no. PLG/2024/017040.

## References

- [1] Agarwal, R., Schwarzer, M., Castro, P. S., Courville, A., and Bellemare, M. G. (2022). Deep Reinforcement Learning at the Edge of the Statistical Precipice.
- [2] Andrychowicz, M., Wolski, F., Ray, A., Schneider, J., Fong, R., Welinder, P., McGrew, B., Tobin, J., Pieter Abbeel, O., and Zaremba, W. (2017). Hindsight experience replay. In Advances in Neural Information Processing Systems, volume 30.
- [3] Ba, J. L., Kiros, J. R., and Hinton, G. E. (2016). Layer Normalization.
- [4] Ball, P. J., Smith, L., Kostrikov, I., and Levine, S. (2023). Efficient online reinforcement learning with offline data. In International Conference on Machine Learning, number arXiv:2302.02948. arXiv.
- [5] Barreto, A., Dabney, W., Munos, R., Hunt, J. J., Schaul, T., van Hasselt, H., and Silver, D. (2022). Successor Features for Transfer in Reinforcement Learning.
- [6] Barto, A. G. (2013). Intrinsic Motivation and Reinforcement Learning. In Baldassarre, G. and Mirolli, M., editors, Intrinsically Motivated Learning in Natural and Artificial Systems, pages 17–47. Springer.
- [7] Baumli, K., Warde-Farley, D., Hansen, S., and Mnih, V. (2021). Relative variational intrinsic control. In Proceedings of the AAAI Conference on Artificial Intelligence, volume 35, pages 6732–6740.
- [8] Bellemare, M. G., Srinivasan, S., Ostrovski, G., Schaul, T., Saxton, D., and Munos, R. (2016). Unifying count-based exploration and intrinsic motivation. In Conference on Neural Information Processing Systems.
- [9] Berseth, G., Geng, D., Devin, C., Rhinehart, N., Finn, C., Jayaraman, D., and Levine, S. (2019). SMiRL: Surprise Minimizing Reinforcement Learning in Unstable Environments. In International Conference on Learning Representations. [object Object].
- [10] Bhargava, P. and Ng, V. (2022). Commonsense Knowledge Reasoning and Generation with Pre-trained Language Models: A Survey.
- [11] Blier, L., Tallec, C., and Ollivier, Y. (2021). Learning Successor States and Goal-Dependent Values: A Mathematical Viewpoint.
- [12] Bonnet, C., Luo, D., Byrne, D., Surana, S., Abramowitz, S., Duckworth, P., Coyette, V., Midgley, L. I., Tegegn, E., Kalloniatis, T., Mahjoub, O., Macfarlane, M., Smit, A. P., Grinsztajn, N., Boige, R., et al. (2024). Jumanji: A diverse suite of scalable reinforcement learning environments in JAX. In International Conference on Learning Representations. arXiv.
- [13] Borsa, D., Barreto, A., Quan, J., Mankowitz, D., Munos, R., van Hasselt, H., Silver, D., and Schaul, T. (2019). Universal successor features approximators. In International Conference on Learning Representations. arXiv.

- [14] Bradbury, J., Frostig, R., Hawkins, P., Johnson, M. J., Leary, C., Maclaurin, D., Necula, G., Paszke, A., VanderPlas, J., Wanderman-Milne, S., and Zhang, Q. (2018). JAX: Composable transformations of Python+NumPy programs.
- [15] Brockman, G., Cheung, V., Pettersson, L., Schneider, J., Schulman, J., Tang, J., and Zaremba, W. (2022). Openai gym. In J. Open Source Softw.
- [16] Calandriello, D., Guo, D., Munos, R., Rowland, M., Tang, Y., Pires, B. A., Richemond, P. H., Lan, C. L., Valko, M., Liu, T., Joshi, R., Zheng, Z., and Piot, B. (2024). Human alignment of large language models through online preference optimisation.
- [17] Chebotar, Y., Hausman, K., Lu, Y., Xiao, T., Kalashnikov, D., Varley, J., Irpan, A., Eysenbach, B., Julian, R., Finn, C., et al. (2021). Actionable models: Unsupervised offline reinforcement learning of robotic skills. In International Conference on Machine Learning.
- [18] Chen, J., Gan, Z., Li, X., Guo, Q., Chen, L., Gao, S., Chung, T., Xu, Y., Zeng, B., Lu, W., Li, F., Carin, L., and Tao, C. (2021). Simpler, faster, stronger: Breaking the log-K curse on contrastive learners with FlatNCE.
- [19] Chen, T., Kornblith, S., Norouzi, M., and Hinton, G. (2020). A Simple Framework for Contrastive Learning of Visual Representations.
- [20] Choi, J., Sharma, A., Lee, H., Levine, S., and Gu, S. S. (2021). Variational empowerment as representation learning for goal-conditioned reinforcement learning. In International Conference on Machine Learning, pages 1953–1963. PMLR.
- [21] Dalton, S., Frosio, I., and Garland, M. (2020). Accelerating reinforcement learning through GPU atari emulation. In Conference on Neural Information Processing Systems. arXiv.
- [22] de Abril, I. M. and Kanai, R. (2018). A unified strategy for implementing curiosity and empowerment driven reinforcement learning.
- [23] Devlin, J., Chang, M.-W., Lee, K., and Toutanova, K. (2019). BERT: Pre-training of deep bidirectional transformers for language understanding. In Annual Conference of the North American Chapter of the Association for Computational Linguistics.
- [24] Ding, W., Lin, H., Li, B., and Zhao, D. (2022). Generalizing Goal-Conditioned Reinforcement Learning with Variational Causal Reasoning. In Conference on Neural Information Processing Systems. arXiv.
- [25] Du, Y., Kosoy, E., Dayan, A., Rufova, M., Abbeel, P., and Gopnik, A. (2023). What can AI learn from human exploration? Intrinsically-motivated humans and agents in open-world exploration. In NeurIPS 2023 Workshop: Information-theoretic Principles in Cognitive Systems.
- [26] Erraqui, A., Machado, M. C., Zhao, M., Sukhbaatar, S., Lazaric, A., Denoyer, L., and Bengio, Y. (2022). Temporal Abstractions-Augmented Temporally Contrastive Learning: An Alternative to the Laplacian in RL.
- [27] Espeholt, L., Marinier, R., Stanczyk, P., Wang, K., and Michalski, M. (2020). SEED RL: Scalable and efficient deep-RL with accelerated central inference. In International Conference on Learning Representations. arXiv.
- [28] Espeholt, L., Soyer, H., Munos, R., Simonyan, K., Mnih, V., Ward, T., Doron, Y., Firoiu, V., Harley, T., Dunning, I., Legg, S., and Kavukcuoglu, K. (2018). IMPALA: Scalable Distributed Deep-RL with Importance Weighted Actor-Learner Architectures. In International Conference on Machine Learning. arXiv.
- [29] Eysenbach, B., Gupta, A., Ibarz, J., and Levine, S. (2019). Diversity is all you need: Learning skills without a reward function. In International Conference on Learning Representations (ICLR).
- [30] Eysenbach, B., Myers, V., Salakhutdinov, R., and Levine, S. (2024). Inference via Interpolation: Contrastive Representations Provably Enable Planning and Inference.
- [31] Eysenbach, B., Salakhutdinov, R., and Levine, S. (2021). C-learning: Learning to achieve goals via recursive classification. In International Conference on Learning Representations. arXiv.
- [32] Eysenbach, B., Zhang, T., Levine, S., and Salakhutdinov, R. R. (2022). Contrastive learning as goal-conditioned reinforcement learning. In Advances in Neural Information Processing Systems, volume 35, pages 35603–35620.
- [33] Farebrother, J., Orbay, J., Vuong, Q., Taiga, A. A., Chebotar, Y., Xiao, T., Irpan, A., Levine, S., Castro, P. S., and Faust, A. (2024). Stop regressing: Training value functions via classification for scalable deep RL. In Forty-First International Conference on Machine Learning, number arXiv:2403.03950. arXiv.

- [34] Fischer, L. G., Silveira, R., and Nedel, L. (2009). Gpu accelerated path-planning for multi-agents in virtual environments. In 2009 VIII Brazilian Symposium on Games and Digital Entertainment, pages 101–110. IEEE.
- [35] Franke, J. K. H., Köhler, G., Biedenkapp, A., and Hutter, F. (2021). Sample-efficient automated deep reinforcement learning. In International Conference on Learning Representations. arXiv.
- [36] Freeman, C. D., Frey, E., Raichuk, A., Girgin, S., Mordatch, I., and Bachem, O. (2021). Brax – a differentiable physics engine for large scale rigid body simulation. In NeurIPS Datasets and Benchmarks. arXiv.
- [37] Fu, J., Kumar, A., Nachum, O., Tucker, G., and Levine, S. (2020). D4rl: Datasets for deep data-driven reinforcement learning.
- [38] Ghosh, D., Gupta, A., and Levine, S. (2019). Learning Actionable Representations with Goal-Conditioned Policies. In International Conference on Learning Representations. arXiv.
- [39] Ghosh, D., Gupta, A., Reddy, A., Fu, J., Devin, C., Eysenbach, B., and Levine, S. (2021). Learning to reach goals via iterated supervised learning. In International Conference on Learning Representations. arXiv.
- [40] Gregor, K., Rezende, D. J., and Wierstra, D. (2016). Variational intrinsic control.
- [41] Gu, S. S., Diaz, M., Freeman, D. C., Furuta, H., Ghasemipour, S. K. S., Raichuk, A., David, B., Frey, E., Coumans, E., and Bachem, O. (2021). Braxlines: Fast and interactive toolkit for RL-driven behavior engineering beyond reward maximization.
- [42] Guan, L., Valmeekam, K., Sreedharan, S., and Kambhampati, S. (2023). Leveraging pre-trained large language models to construct and utilize world models for model-based task planning. In Advances in Neural Information Processing Systems, volume 36, pages 79081–79094.
- [43] He, K., Chen, X., Xie, S., Li, Y., Dollár, P., and Girshick, R. (2022). Masked autoencoders are scalable vision learners. In IEEE/CVF Conference on Computer Vision and Pattern Recognition. arXiv.
- [44] Heek, J., Levskaya, A., Oliver, A., Ritter, M., Rondepierre, B., Steiner, A., and van Zee, M. (2023). Flax: A neural network library and ecosystem for JAX.
- [45] Henderson, P., Islam, R., Bachman, P., Pineau, J., Precup, D., and Meger, D. (2018). Deep reinforcement learning that matters. In Proceedings of the AAAI Conference on Artificial Intelligence. arXiv.
- [46] Hennigan, T., Cai, T., Norman, T., Martens, L., and Babuschkin, I. (2020). Haiku: Sonnet for JAX.
- [47] Hoang, C., Sohn, S., Choi, J., Carvalho, W., and Lee, H. (2021). Successor feature landmarks for long-horizon goal-conditioned reinforcement learning. In Advances in Neural Information Processing Systems, volume 34, pages 26963–26975. Curran Associates, Inc.
- [48] Hoffman, M. W., Shahriari, B., Aslanides, J., Barth-Maron, G., Momchev, N., Sinopalnikov, D., Stańczyk, P., Ramos, S., Raichuk, A., Vincent, D., Hussenot, L., Dadashi, R., Dulac-Arnold, G., Orsini, M., Jacq, A., et al. (2022). Acme: A research framework for distributed reinforcement learning.
- [49] Hoffmann, J., Borgeaud, S., Mensch, A., Buchatskaya, E., Cai, T., Rutherford, E., Casas, D. d. L., Hendricks, L. A., Welbl, J., Clark, A., Hennigan, T., Noland, E., and Millican, K. (2022). Training compute-optimal large language models.
- [50] Hu, T., Liu, Z., Zhou, F., Wang, W., and Huang, W. (2023). Your contrastive learning is secretly doing stochastic neighbor embedding. In International Conference on Learning Representations. arXiv.
- [51] Jin, Z., Chen, Y., Leeb, F., Gresle, L., Kamal, O., Zhiheng, L. Y. U., Blin, K., Adauto, F. G., Kleiman-Weiner, M., and Sachan, M. (2023). Cladder: Assessing causal reasoning in language models. In Thirty-Seventh Conference on Neural Information Processing Systems.
- [52] Jordan, S., Chandak, Y., Cohen, D., Zhang, M., and Thomas, P. (2020). Evaluating the performance of reinforcement learning algorithms. In International Conference on Machine Learning, pages 4962–4973. PMLR.
- [53] Jordan, S. M., White, A., da Silva, B. C., White, M., and Thomas, P. S. (2024). Position: Benchmarking is limited in reinforcement learning research.
- [54] Kaelbling, L. P. (1993). Learning to Achieve Goals. In International Joint Conference on Artificial Intelligence.

- [55] Kim, J., Park, S., and Kim, G. (2021). Unsupervised Skill Discovery with Bottleneck Option Learning. In International Conference on Machine Learning. arXiv.
- [56] Klyubin, A. S., Polani, D., and Nehaniv, C. L. (2005). Empowerment: A universal agent-centric measure of control. In 2005 IEEE Congress on Evolutionary Computation, volume 1, pages 128–135. IEEE.
- [57] Koyamada, S., Okano, S., Nishimori, S., Murata, Y., Habara, K., Kita, H., and Ishii, S. (2023). Pgx: Hardware-accelerated parallel game simulators for reinforcement learning. 36:45716–45743.
- [58] Kwon, M., Hu, H., Myers, V., Karamcheti, S., Dragan, A., and Sadigh, D. (2023). Toward Grounded Commonsense Reasoning. In International Conference on Robotics and Automation (ICRA). arXiv.
- [59] Laskin, M., Liu, H., Peng, X. B., Yarats, D., Rajeswaran, A., and Abbeel, P. (2022). CIC: Contrastive Intrinsic Control for Unsupervised Skill Discovery.
- [60] Levine, S. and Shah, D. (2023). Learning Robotic Navigation from Experience: Principles, Methods, and Recent Results. 378(1869):20210447.
- [61] Liang, J., Makoviychuk, V., Handa, A., Chentanez, N., Macklin, M., and Fox, D. (2018). GPU-accelerated robotic simulation for distributed reinforcement learning. In Proceedings of The 2nd Conference on Robot Learning, pages 270–282. PMLR.
- [62] Lillicrap, T. P., Hunt, J. J., Pritzel, A., Heess, N., Erez, T., Tassa, Y., Silver, D., and Wierstra, D. (2016). Continuous control with deep reinforcement learning. In International Conference on Learning Representations.
- [63] Liu, B., Feng, Y., Liu, Q., and Stone, P. (2023). Metric Residual Network for Sample Efficient Goal-Conditioned Reinforcement Learning. In Proceedings of the AAAI Conference on Artificial Intelligence, volume 37, pages 8799–8806.
- [64] Ma, Y. J., Liang, W., Som, V., Kumar, V., Zhang, A., Bastani, O., and Jayaraman, D. (2023). LIV: Language-image representations and rewards for robotic control. In International Conference on Machine Learning. arXiv.
- [65] Makoviychuk, V., Wawrzyniak, L., Guo, Y., Lu, M., Storey, K., Macklin, M., Hoeller, D., Rudin, N., Allshire, A., Handa, A., and State, G. (2021). Isaac gym: High performance GPU-based physics simulation for robot learning. In NeurIPS Datasets and Benchmarks. arXiv.
- [66] Manderson, T., Higuera, J. C. G., Wapnick, S., Tremblay, J.-F., Shkurti, F., Meger, D., and Dudek, G. (2020). Vision-based goal-conditioned policies for underwater navigation in the presence of obstacles.
- [67] Matthews, M., Beukman, M., Ellis, B., Samvelyan, M., Jackson, M. T., Coward, S., and Foerster, J. N. (2024). Craftax: A Lightning-Fast Benchmark for Open-Ended Reinforcement Learning. In Forty-First International Conference on Machine Learning.
- [68] Mikolov, T., Sutskever, I., Chen, K., Corrado, G. S., and Dean, J. (2013). Distributed representations of words and phrases and their compositionality. In Advances in Neural Information Processing Systems, volume 26. Curran Associates, Inc.
- [69] Mittal, S. and Vaishay, S. (2019). A survey of techniques for optimizing deep learning on GPUs.
- [70] Mnih, V., Badia, A. P., Mirza, M., Graves, A., Lillicrap, T. P., Harley, T., Silver, D., and Kavukcuoglu, K. (2016). Asynchronous methods for deep reinforcement learning. In International Conference on Machine Learning.
- [71] Mnih, V., Kavukcuoglu, K., Silver, D., Rusu, A. A., Veness, J., Bellemare, M. G., Graves, A., Riedmiller, M., Fidjeland, A. K., Ostrovski, G., Petersen, S., Beattie, C., Sadik, A., Antonoglou, I., King, H., et al. (2015). Human-level control through deep reinforcement learning. 518(7540):529–533.
- [72] Muennighoff, N., Rush, A., Barak, B., Le Scao, T., Tazi, N., Piktus, A., Pyysalo, S., Wolf, T., and Raffel, C. A. (2023). Scaling data-constrained language models. In Advances in Neural Information Processing Systems, volume 36, pages 50358–50376.
- [73] Myers, V., Ellis, E., Eysenbach, B., Levine, S., and Dragan, A. (2024a). Learning to Assist Humans without Inferring Rewards. In ICML 2024 Workshop on Models of Human Feedback for AI Alignment.
- [74] Myers, V., He, A. W., Fang, K., Walke, H. R., Hansen-Estruch, P., Cheng, C.-A., Jalobeanu, M., Kolobov, A., Dragan, A., and Levine, S. (2023). Goal Representations for Instruction Following: A Semi-Supervised Language Interface to Control. In Proceedings of The 7th Conference on Robot Learning, pages 3894–3908. PMLR.

- [75] Myers, V., Zheng, C., Dragan, A., Levine, S., and Eysenbach, B. (2024b). Learning Temporal Distances: Contrastive Successor Features Can Provide a Metric Structure for Decision-Making. In International Conference on Machine Learning, number arXiv:2406.17098. arXiv.
- [76] Nachum, O., Gu, S. S., Lee, H., and Levine, S. (2018). Data-efficient hierarchical reinforcement learning.
- [77] Nair, A. V., Pong, V., Dalal, M., Bahl, S., Lin, S., and Levine, S. (2018). Visual reinforcement learning with imagined goals. In Advances in Neural Information Processing Systems, volume 31. Curran Associates, Inc.
- [78] Nauman, M., Bortkiewicz, M., Miłoś, P., Trzcinski, T., Ostaszewski, M., and Cygan, M. (2024). Overestimation, overfitting, and plasticity in actor-critic: The bitter lesson of reinforcement learning. In Forty-First International Conference on Machine Learning, number arXiv:2403.00514. arXiv.
- [79] Park, S., Choi, J., Kim, J., Lee, H., and Kim, G. (2021). Lipschitz-constrained Unsupervised Skill Discovery. In International Conference on Learning Representations.
- [80] Park, S., Ghosh, D., Eysenbach, B., and Levine, S. (2023). HIQL: Offline Goal-Conditioned RL with Latent States as Actions. In Conference on Neural Information Processing Systems. arXiv.
- [81] Park, S., Rybkin, O., and Levine, S. (2024). METRA: Scalable Unsupervised RL with Metric-Aware Abstraction. In International Conference on Learning Representations. arXiv.
- [82] Radford, A., Kim, J. W., Hallacy, C., Ramesh, A., Goh, G., Agarwal, S., Sastry, G., Askell, A., Mishkin, P., Clark, J., Krueger, G., and Sutskever, I. (2021). Learning Transferable Visual Models From Natural Language Supervision.
- [83] Rajani, N. F., McCann, B., Xiong, C., and Socher, R. (2019). Explain Yourself! Leveraging Language Models for Commonsense Reasoning. In Proceedings of the 57th Annual Meeting of the Association for Computational Linguistics, pages 4932–4942. Association for Computational Linguistics.
- [84] Rauber, P., Ummadisingu, A., Mutz, F., and Schmidhuber, J. (2021). Hindsight policy gradients. In Neural Comput. arXiv.
- [85] Rhinehart, N., Wang, J., Berseth, G., Co-Reyes, J., Hafner, D., Finn, C., and Levine, S. (2021). Information is Power: Intrinsic Control via Information Capture. In Advances in Neural Information Processing Systems, volume 34, pages 10745–10758. Curran Associates, Inc.
- [86] Rutherford, A., Ellis, B., Gallici, M., Cook, J., Lupu, A., Ingvarsson, G., Willi, T., Khan, A., de Witt, C. S., and Souly, A. (2024). JaxMARL: Multi-agent RL environments in JAX. In Second Agent Learning in Open-Endedness Workshop.
- [87] Salge, C., Glackin, C., and Polani, D. (2013). Empowerment – an Introduction.
- [88] Sardana, N., Portes, J., Doubov, S., and Frankle, J. (2024). Beyond chinchilla-optimal: Accounting for inference in language model scaling laws. In International Conference on Machine Learning. arXiv.
- [89] Schaul, T., Horgan, D., Gregor, K., and Silver, D. (2015). Universal Value Function Approximators. In Proceedings of the 32nd International Conference on Machine Learning, pages 1312–1320.
- [90] Schulman, J., Moritz, P., Levine, S., Jordan, M., and Abbeel, P. (2015). High-dimensional continuous control using generalized advantage estimation.
- [91] Sermanet, P., Lynch, C., Hsu, J., and Levine, S. (2017). Time-Contrastive Networks: Self-Supervised Learning from Multi-view Observation. In 2017 IEEE Conference on Computer Vision and Pattern Recognition Workshops (CVPRW), pages 486–487.
- [92] Shah, D., Sridhar, A., Dashora, N., Stachowicz, K., Black, K., Hirose, N., and Levine, S. (2023). ViNT: A Foundation Model for Visual Navigation. In Conference on Robot Learning. arXiv.
- [93] Sharma, A., Gu, S., Levine, S., Kumar, V., and Hausman, K. (2020). Dynamics-aware unsupervised discovery of skills. In International Conference on Learning Representations.
- [94] Silver, D., Huang, A., Maddison, C. J., Guez, A., Sifre, L., van den Driessche, G., Schrittwieser, J., Antonoglou, I., Panneershelvam, V., Lanctot, M., Dieleman, S., Grewe, D., Nham, J., Kalchbrenner, N., Sutskever, I., et al. (2016). Mastering the game of go with deep neural networks and tree search. 529(7587):484–489.

- [95] Silver, D., Hubert, T., Schrittwieser, J., Antonoglou, I., Lai, M., Guez, A., Lanctot, M., Sifre, L., Kumaran, D., Graepel, T., Lillicrap, T., Simonyan, K., and Hassabis, D. (2017). Mastering chess and shogi by self-play with a general reinforcement learning algorithm.
- [96] Sohn, K. (2016). Improved deep metric learning with multi-class N-pair loss objective. In Advances in Neural Information Processing Systems, volume 29. Curran Associates, Inc.
- [97] Sukhbaatar, S., Lin, Z., Kostrikov, I., Synnaeve, G., Szlam, A., and Fergus, R. (2018). Intrinsic motivation and automatic curricula via asymmetric self-play. In International Conference on Learning Representations.
- [98] Tassa, Y., Doron, Y., Muldal, A., Erez, T., Li, Y., Casas, D. d. L., Budden, D., Abdolmaleki, A., Merel, J., Lefrancq, A., Lillicrap, T., and Riedmiller, M. (2018). DeepMind control suite.
- [99] Tassa, Y., Erez, T., and Todorov, E. (2012). Synthesis and stabilization of complex behaviors through online trajectory optimization. In 2012 IEEE/RSJ International Conference on Intelligent Robots and Systems, pages 4906–4913. IEEE.
- [100] Thibault, W., Melek, W., and Mombaur, K. (2024). Learning velocity-based humanoid locomotion: Massively parallel learning with brax and MJX.
- [101] Touati, A. and Ollivier, Y. (2021). Learning One Representation to Optimize All Rewards.
- [102] Tunyasuvunakool, S., Muldal, A., Doron, Y., Liu, S., Bohez, S., Merel, J., Erez, T., Lillicrap, T., Heess, N., and Tassa, Y. (2020). dm\_control: Software and tasks for continuous control. 6:100022.
- [103] Valmeekam, K., Olmo, A., Sreedharan, S., and Kambhampati, S. (2022). Large language models still can’t plan (a benchmark for LLMs on planning and reasoning about change). In NeurIPS 2022 Foundation Models for Decision Making Workshop.
- [104] van den Oord, A., Li, Y., and Vinyals, O. (2019). Representation Learning with Contrastive Predictive Coding.
- [105] Venkattaramanujam, S., Crawford, E., Doan, T., and Precup, D. (2020). Self-supervised learning of distance functions for goal-conditioned reinforcement learning.
- [106] Walke, H. R., Black, K., Zhao, T. Z., Vuong, Q., Zheng, C., Hansen-Estruch, P., He, A. W., Myers, V., Kim, M. J., Du, M., Lee, A., Fang, K., Finn, C., and Levine, S. (2023). BridgeData V2: A Dataset for Robot Learning at Scale. In Conference on Robot Learning, pages 1723–1736. PMLR.
- [107] Wang, T., Torralba, A., Isola, P., and Zhang, A. (2023). Optimal goal-reaching reinforcement learning via quasimetric learning. In International Conference on Machine Learning. arXiv.
- [108] Wawrzyński, P. (2009). A Cat-Like Robot Real-Time Learning to Run. In Kolehmainen, M., Toivanen, P., and Beliczynski, B., editors, Adaptive and Natural Computing Algorithms, pages 380–390. Springer.
- [109] Zha, D., Xie, J., Ma, W., Zhang, S., Lian, X., Hu, X., and Liu, J. (2021). DouZero: Mastering DouDizhu with self-play deep reinforcement learning. In Proceedings of the 38th International Conference on Machine Learning, pages 12333–12344. PMLR.
- [110] Zheng, C., Eysenbach, B., Walke, H., Yin, P., Fang, K., Salakhutdinov, R., and Levine, S. (2024). Stabilizing Contrastive RL: Techniques for Offline Goal Reaching. In International Conference on Learning Representations. arXiv.
- [111] Zheng, C., Salakhutdinov, R., and Eysenbach, B. (2023). Contrastive Difference Predictive Coding. In The Twelfth International Conference on Learning Representations. arXiv.
- [112] Zhu, Y., Min, M. R., Kadav, A., and Graf, H. P. (2020). S3vae: Self-supervised sequential vae for representation disentanglement and data generation. In Proceedings of the IEEE/CVF Conference on Computer Vision and Pattern Recognition, pages 6538–6547.

## A Experimental Details

### A.1 Speedup comparison across various numbers of parallel environments

We present an extended version of the plot from Fig. 1, with additional experiments, as depicted on the left side of Fig. 10. Each experiment was run for 10M environment steps, and for the original repository, we varied the number of parallel actors for data collection, testing configurations with 4, 8, 16, and 32 actors, each running on separate CPU threads. Each configuration was tested with three different random seeds, and we present the results along with the corresponding standard deviations. The novel repository used 1024 actors for data collection.

A notable observation from these experiments is the variation in success rates associated with different numbers of parallel actors. We hypothesize that this discrepancy arises due to the increased diversity of data supplied to the replay buffer as the number of independent parallel environments increases, leading to more varied experiences for each policy update. To further investigate, we conducted similar experiments using our method with varying numbers of parallel environments. The results are presented on the right side of Fig. 10. This observation, while interesting, is beyond the scope of the current work and is proposed as an area for further investigation.

Additionally, we repeated these experiments for the Ant U-Maze environment. The results are shown in Fig. 11. The speedup provided by our novel repository is clearly evident from the figure. Although the asymptotic performance of proposed and original CRL repositories differ, it is important to consider that the physical backends used for Ant-Umaze differ between the repositories, and Brax is still under active development. These discrepancies likely contribute to the observed differences in success rates. We anticipate that future versions will exhibit reduced performance discrepancies.

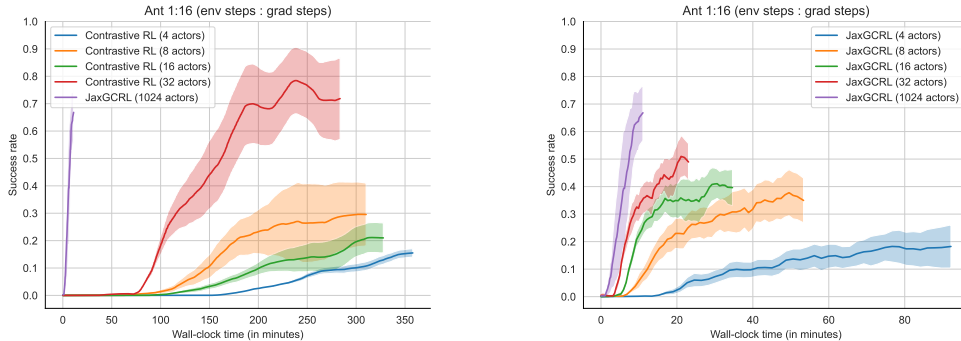


Figure 10: Speedup in ant environment for the 1:16 ratio of SGD steps : environment steps for different numbers of parallel actors.

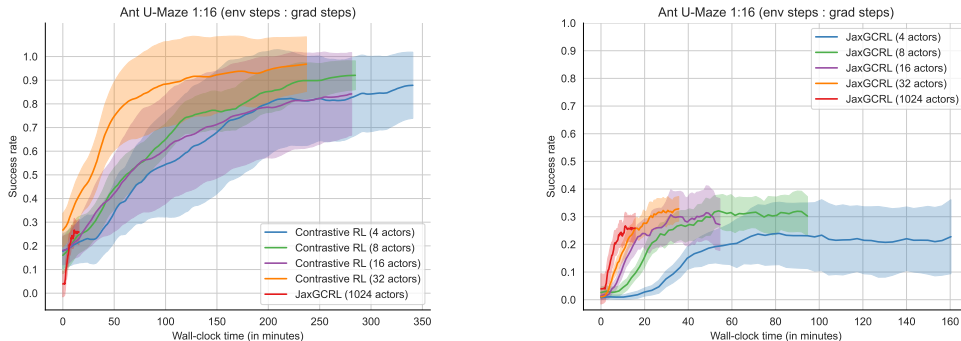


Figure 11: Speedup in ant u-maze environment for the 1:16 ratio of SGD steps : environment steps for different numbers of parallel actors.

## A.2 Energy functions

Figure 12 shows the results of different energy functions per environment, success rate and time near goal. Clearly, no single energy function performs well in all the tested environments, as, for instance, L1 and L2, which perform well in Ant environments, work poorly in Pusher. In addition, we observed high variability in every configuration performance, as indicated by relatively wide standard errors.

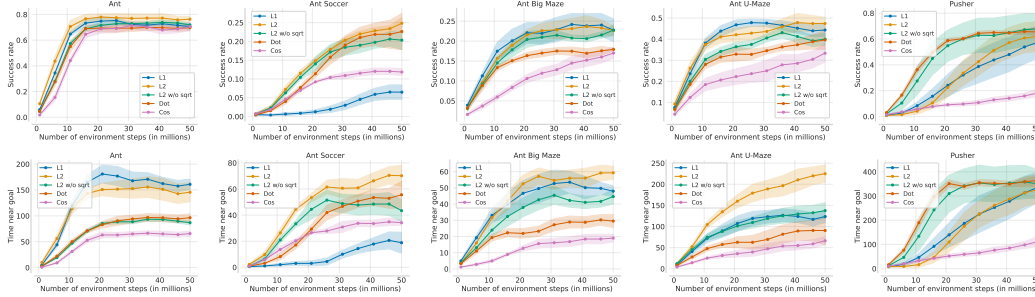


Figure 12: Success rate (top) and time near goal (bottom) results in different energy functions and environments. Best performing energy function varies across environments.

## B Technical details

### B.1 Environment details

In each of the environments there are a number of parameters that can change the learning process. A non-exhaustive list of such details for each environment is presented below.

Table 1: Environments details

| Environment  | Goal distance    | Termination | Brax pipeline | Goal sampling   |
|--------------|------------------|-------------|---------------|---|
| Reacher      | 0.05             | No          | Spring        | Disc with radius sampled from $[0.0, 0.2]$  |
| Half-Cheetah | 0.5              | No          | MJX           | Fixed goal location   |
| Pusher Easy  | 0.1              | No          | Generalized   | x coordinate sampled from $[-0.55, -0.25]$ , y coordinate sampled from $[-0.2, 0.2]$  |
| Pusher Hard  | 0.1              | No          | Generalized   | x coordinate sampled from $[-0.65, 0.35]$ , y coordinate sampled from $[-0.55, 0.45]$ |
| Humanoid     | 0.5 <sup>1</sup> | Yes         | Spring        | Disc with radius sampled from $[1.0, 5.0]$ ( $[5.0, 5.0]$ <b>for evaluation</b> )     |
| Ant          | 0.5              | Yes         | Spring        | Circle with radius 10.0   |
| Ant Maze     | 0.5              | Yes         | Spring        | Maze specific   |
| Ant Soccer   | 0.5              | Yes         | Spring        | Circle with radius 5.0  |
| Ant Push     | 0.5              | Yes         | MJX           | Two possible locations with uniform noise added                                       |

### B.2 Benchmark parameters

The parameters used for benchmarking experiments can be found in Table 2:

<sup>1</sup>in 3 dimensions

Table 2: Hyperparameters

| Hyperparameter                              | Value                    |
|---|--------------------------|
| num_timesteps                               | 50,000,000               |
| max_replay_size                             | 10,000                   |
| min_replay_size                             | 1,000                    |
| episode_lenght                              | 1,000                    |
| discounting                                 | 0.99                     |
| num_envs                                    | 1024 (512 for humanoid)  |
| batch_size                                  | 256                      |
| multiplier_num_sgd_steps                    | 1                        |
| action_repeat                               | 1                        |
| unroll_length                               | 62                       |
| policy_lr                                   | 6e-4                     |
| critic_lr                                   | 3e-4                     |
| contrastive_loss_function                   | symmetric_infonce        |
| energy_function                             | L2                       |
| logsumexp_penalty                           | 0.1                      |
| hidden layers (for both encoders and actor) | [1024, 1024, 1024, 1024] |
| representation dimension                    | 64                       |

## C Random Goals

Our loss in Eq. (2) differs from the original CRL algorithm [32] by sampling goals from the same trajectories as states during policy extraction, rather than random goals from the replay buffer. Mathematically, we can generalize Eq. (2) to account for either of these strategies by adding a hyperparameter  $\alpha$  to the loss controlling the degree of random goal sampling during training.

$$\mathcal{L}_{\text{policy}}(\mathcal{B}; \theta) = \sum_{i,j=1}^K \int_{\mathcal{A}} (1 - \alpha) f_{\phi, \psi}(s_i, a_i, g_i) d\pi_{\theta}(a_i | s_i, g_i) \quad (17)$$

$$+ \alpha f_{\phi, \psi}(s_i, a_i, g_j) d\pi_{\theta}(a_i | s_i, g_j). \quad (18)$$

The hyperparameter  $\alpha$  controls the rate of counterfactual goal learning, where the policy is updated based on the critic’s evaluation of goals that did not actually occur in the trajectory. We find that taking,  $\alpha = 0$  (i.e., no random goal sampling) leads to better performance, and suggest using the policy loss in Eq. (2) for training contrastive RL methods.

We use a DDPG-style policy extraction loss to learn a goal-conditioned policy with this critic [62]. Parameterizing the policy as some  $\pi_{\theta}(a | s, g)$ , we get